Mon. Not. R. Astron. Soc. **362,** 957–965 (2005) doi:10.1111/j.1365-2966.2005.09368.x

SS 433: results of a recent multiwavelength campaign

Sandip K. Chakrabarti,[1,2⋆] B. G. Anandarao,[3⋆] S. Pal,[2⋆] Soumen Mondal,[3⋆] A. Nandi,[1,2⋆] A. Bhattacharyya,[2⋆] Samir Mandal,[2⋆] Ram Sagar,[4⋆] J. C. Pandey,[4⋆] A. Pati[5⋆] and S. K. Saha[5⋆]

[1]*S. N. Bose National Center for Basic Sciences, JD-Block, Salt Lake, Kolkata, 700098, India*
[2]*Centre for Space Physics, Chalantika 43, Garia Station Rd., Kolkata, 700084, India*
[3]*Physical Research Laboratory, Navarangapura, Ahmedabad, 380009, India*
[4]*ARIES, Manora Peak, Nainital, 263129, India*
[5]*Indian Institute of Astrophysics, Bangalore 560034, India*

Accepted 2005 June 27. Received 2005 June 27; in original form 2004 December 31

ABSTRACT

We conducted a multiwavelength campaign in 2002 September–October, to observe SS 433. We used the Giant Meter Radio Telescope for radio observations, the Physical Research Laboratory Infrared Telescope at Mt Abu for infrared (IR), the ARIES telescope at Nainital for optical photometry, the telescope at the Vainu Bappu observatory for spectral measurements and the *Rossi X-ray Timing Explorer* for X-ray observations. We find sharp variations in intensity on time-scales of a few minutes in the X-ray, IR and radio wavelengths. Differential photometry in the IR observations clearly indicates significant intrinsic variations on short time-scales of minutes throughout the campaign. Combining the results for these wavelengths, we find a signature of delay of about two days between the IR and radio signals. The X-ray spectrum yielded double Fe line profiles which corresponded to red and blue components of the relativistic jet. We also present the broad-band spectrum averaged over the campaign duration.

Key words: methods: miscellaneous – stars: individual: SS 433 – stars: winds, outflows – infrared: stars – radio continuum: stars – X-rays: stars.

1 INTRODUCTION

The enigmatic compact star SS 433 is a well-studied bright emission-line object which is known to have a companion with an orbital period of 13.1 d, a large disc and two highly collimated relativistic jets moving at $v \sim 0.26$ c. The disc axis makes an angle of $\sim 78^\circ$ with the line of sight, while the jet precesses with the axis at an angle of $\sim 19^\circ$ (Margon 1984) with a periodicity of about 162.15 d. Several observations have been carried out over the last three decades, yet the object has eluded a proper identification. Most recent estimates (Hillwig et al. 2004) suggest that the central object could be a low-mass black hole ($2.9 \pm 0.7\ M_\odot$) with a high-mass ($10.9 \pm 3.1\ M_\odot$) companion.

While there are many truly multiwavelength campaigns ranging from radio emission to gamma rays for 'active' microquasars such as GRS 1915+105 (Ueda et al. 2002; Fuchs et al. 2003) or GX339-4 (Corbel et al. 2003; Homan et al. 2005), so far the campaigns for SS 433 are confined to only two or three wavelengths (e.g. Neizvestnyj et al. 1980; Ciatti et al. 1981; Seaquist et al. 1982; Vermeulen 1989; Band & Gordon 1989; Kotani et al. 1999; Revnivtsev et al. 2004). The problem with SS 433 is that there is a large amount of gas from the companion which surrounds the disc and blocks the disc emission of X-rays. Thus, it is not as 'exciting' a source as other microquasars as far as X-ray properties are concerned. Revnivtsev et al. (2004) found that SS 433 exhibited chaotic optical variability on time-scales of as small as 10 s. Fuchs et al. (2001) found evidence of synchrotron emission in infrared (IR) radiation in the western lobe of SS 433. Earlier, Milone & Clark (1979) and Glass (1979) also reported IR variability in time-scales of minutes. Gies et al. (2002) obtained various spectral components of SS 433, mostly concentrating on the optical and ultraviolet (UV) spectrometry.

The aim of our campaign on SS 433 was (a) to carry out observations in as many wavelengths as possible, (b) to detect the nature of the short time-scale variabilities in all the wavelengths, and (c) to obtain a broad-band spectrum of this enigmatic system in order to model the emission processes in future. We carried out the campaign in radio (1.28 GHz), in IR (J, H, and K' bands), in optical (B and V bands) and in X-ray (3–30 keV) wavelengths in 2002 September–October, when the jet was more or less normal to the line of sight and the X-ray intensity was statistically at its minimum. Given that the jet is produced out of matter ejected from the accretion disc, one would expect that small variabilities, if present, would exist in all the wavelengths and one would hope to correlate these variabilities in order to 'follow' individual flares or knots as they propagate through the jets. We did observe such variabilities in time-scales of a few

⋆E-mail: chakraba@bose.res.in (SKC); anand@prl.ernet.in (BGA); space_phys@vsnl.com (SP, SM, AB); soumen@prl.ernet.in (SM); anuj@bose.res.in (AN); sagar@upso.ernet.in (RS); jeewan@upso.ernet.in (JCP); pati@iiap.res.in (AP); sks@iiap.res.in (SKS)

minutes, but given that quite 'unknown' time delays are present between X-rays and optical, IR or radio-emitting regions, we found it difficult to correlate these variabilities. However, we did find a lag of almost two days between the overall variation of intensities in the IR and radio emissions. Our radio observation was carried out during 2002 September 26 to October 6. The IR observations took place during 2002 September 25–29, the optical photometry during 2002 September 27 to October 3, and X-ray observation only on 2002 September 27. Optical spectra were taken on 2002 September 27 and 28. A brief report on the variabilities in radio, IR and X-rays, observed on 2002 September 27 has already been published in Chakrabarti et al. (2003).

In the following Sections, we present the results of our multiwavelength campaign. In Section 2, we briefly describe the observations and the data reduction. In Section 3, we present our results including the light curve and the broad-band spectrum. Finally, in Section 4, we draw our conclusions.

2 OBSERVATIONS AND DATA REDUCTION

Table 1 gives a log of our observations during the campaign and brief remarks on each observation. Column 1 gives Modified Julian Day (MJD) and the date of observation, Column 2 the wave band, and Column 3 the telescope used and its location. For the Giant Meter Radio Telescope (GMRT), we also give (in square brackets) the number of antennas working during the observation. Column 4 gives the duration of the observations in seconds.

Table 1. Observation log of SS 433.

MJD (Date)	Waveband	Telescope (location)	Duration (s)
52542 (25/9/02)	*J*	PRL(Mt. Abu)	1480
	H	PRL(Mt. Abu)	1720
	K′	PRL(Mt. Abu)	740
52543 (26/9/02)	1.28 GHz	GMRT(Pune) [20][a)]	2160
	J	PRL(Mt. Abu)	3640
52544(27/9/02)	1.28 GHz	GMRT(Pune) [28]	21600
	J	PRL(Mt. Abu)	2500
	H	PRL(Mt. Abu)	2390
	K′	PRL(Mt. Abu)	2180
	B	State Obs.(Nainital)	1320
	Optical	VBT (Kavalur)	2400
	spectroscopy	VBT (Kavalur)	2400
	3–30 keV	*RXTE*	5696
52545(28/9/02)	1.28 GHz	GMRT(Pune) [24]	960
	B	State Obs. (Nainital)	4860
	Optical	VBT (Kavalur)	3900
	spectroscopy	VBT (Kavalur)	3900
52546(29/9/02)	1.28 GHz	GMRT(Pune) [13]	840
	J	PRL(Mt. Abu)	1160
	H	PRL(Mt. Abu)	780
	K′	PRL(Mt. Abu)	475
52547(30/9/02)	1.28 GHz	GMRT(Pune) [26]	24024
52548(1/10/02)	1.28 GHz	GMRT(Pune) [28]	16027
52549(2/10/02)	1.28 GHz	GMRT(Pune) [28]	6689
52550(3/10/02)	*B*	State Obs. (Nainital)	120
	V	State Obs. (Nainital)	120
52552(5/10/02)	610 MHz	GMRT(Pune) [29]	1130
52553(6/10/02)	610 MHz	GMRT(Pune) [10]	2850

(*a*)The number of antennas working during the observation.

Radio observations were carried out with GMRT. For a description, see Chakrabarti et al. (2003). The observation was carried out at 1.280 GHz (bandwidth 16 MHz) during 2002 September 26 to October 1 and at 610 MHz (bandwidth 16 MHz) during 2002 October 2–6. However, the observations of 2002 October 3–4 were severely affected by scintillation. These data were not used. The remaining data were stored after binning at every 16 s during acquisition. The National Radio Astronomy Observatory's AIPS package was used to reduce the data. Bad data were flagged and good data were band-passed and channel averaged. The time variation of flux of the source was found and the standard deviation in each time bin was computed. Generally, 2011-067 and 1925+211 were used as phase calibrators and 3C48 and 3C286 were used as flux calibrators whenever available.

Infrared observations were made using the Physical Research Laboratory (PRL) 1.2 m Mt. Abu infrared telescope equipped with the Near Infrared Camera and Multi-Object Spectrometer (NICMOS). For a full description, see Chakrabarti et al. (2003). One pixel corresponds to 0.47 arcsec on the sky, giving a field of view of 2×2 arcmin^2. Short exposures were taken in immediate succession in standard J, H and K' bands. Single-frame exposure times during whole observations in the J and H filters were 10 s. Observations in the K' filter were taken with 2-s exposures and five successive frames were binned to obtain 10 s for a better signal-to-noise ratio. On 2002 September 26 only J band observation could be made before clouds covered the sky. At each dithered position, ten frames were taken with each integration time of 10 s. The nearby infrared bright standard star GL748 (Elias et al. 1982) was used as the flux calibrator and it was observed for 50 frames with exposure time of 10 s in each filter during each night.

Data reduction of JHK' images were performed in a standard way using the DAOPHOT task of the IRAF package. All the objects and standard star frames were de-biased, sky-subtracted and flat fielded. The sky frames were created by the usual practice of the median combining of at least five position-dithered images where the source was kept within the field of NICMOS of $2' \times 2'$. At each dithered position at least 10 frames of 10-s exposure were taken for J and H bands while 20 frames of 2-s exposure were taken for K' band. The zero point of the instrument was taken from the standard star observation. We measured the stellar magnitudes using the aperture photometry task (APPHOT) in IRAF. Our derived mean JHK' magnitudes on 2002 September 25, 27 and 29 were 9.51 ± 0.04, 8.48 ± 0.03 and 8.49 ± 0.08; 9.47 ± 0.02, 8.48 ± 0.02 and 8.32 ± 0.02; 9.51 ± 0.01, 8.49 ± 0.04 and 8.38 ± 0.03 respectively. On September 26, the J magnitude was 9.52 ± 0.02 . The magnitudes were converted to flux density (Jansky) using the zero-magnitude flux scale of Bessell et al. (1998) for plotting purpose. The differential magnitudes were determined using the two brightest stars in the same frame of the object. The error in individual flux density measurement is the usual propagation error of the observed photometric magnitude. Photometric errors ϵ were calculated for individual frames of every star and for the subtracted differential magnitude the final error was calculated as $\sqrt{\epsilon_1^2 + \epsilon_2^2}$, where ϵ_1 and ϵ_2 are the error-bars of the individual stars.

The optical photometry was carried out at the State Observatory (currently known as the Aryabhatta Research Institute of Observational Sciences or ARIES), Nainital, India using its 1-m reflector.

The photometric observations in Johnson B and V bands were carried out using a CCD camera at the f/13 Cassegrain focus of the telescope. The CCD system consists of $24 \times 24\,\mu^2$ size pixels, having 2048×2048 pixels. To improve the signal-to-noise ratio the observations were taken in a binning mode of 2×2 pixel^2, where each super pixel corresponded to 0.72×0.72 arcsec^2. The CCD covers a field of view of $\sim 13 \times 13$ arcmin^2. Multiple CCD frames were taken with the exposure time of 120 s. A number of bias and twilight flat-field frames were also taken during the observing run. The frames were cleaned employing the IRAF/Munich Image Data Analysis System (MIDAS) software. The magnitude of the star was determined by using DAOPHOT. The value of atmospheric extinction in the B passband was 0.26 during the observation and this was taken into account. Because of scattered clouds, only a few exposures could be made on 2002 September 27, and only one exposure on each of the B and V bands could be made on 2002 October 3. Several exposures were taken on 2002 September 28.

The optical spectroscopic study of SS 433 was carried out with the 2.3-m Vainu Bappu Telescope (VBT) at the Vainu Bappu Observatory (VBO), Kavalur, India. CCD images were obtained during the period of 2002 September 27–28. Detailed descriptions of the telescope characteristics and observation techniques are given in Prabhu et al. (1995). The source was pointed at for a maximum exposure time of 20 min with the source positioned at the centre of the CCD frame. The data were analysed with PC-IRAF 2.12.1-EXPORT version. The processing involved to obtain the spectra is comprised of several subroutines which were performed in a pipe-line. These include (a) making the MASTERBIAS using all the bias files supplied with the data with the *median combine* option; (b) making the MASTERFLAT using all flat files supplied with data with the *median combine* option; (c) checking one of the flat files to get the range of useful data; (d) using CCDPROC on all the science and science calibration files to correct for bias, flat-fielding, and the trimming out of noise; (e) removal of the cosmic rays using the COSMICRAYS utility; (f) performing the aperture synthesis of science data after checking the dispersion axis and matching with the APALL parameters; (g) using APALL for the science calibration file to calibrate with the proper science data; (h) calibration of spectrum lines in the calibration data; (i) wavelength calibration (non-linear) of the science data file using the science calibrator file with *dispcor*, and finally, (j) the continuum calibration of the wavelength calibrated science data. Since we did not have a standard spectrum (due to bad weather), we could not perform an absolute flux calibration and so we had to rely on the simple continuum calibrated data. Iron and Neon lines were used to calibrate lines.

X-ray observations were carried out using the Proportional Counter Array (PCA) aboard the *RXTE* satellite. The data reduction and analysis were performed using software LHEASOFT, FTOOLS 5.1 and XSPEC 11.1. We extracted light curves from the *RXTE* PCA Science Data in GoodXenon mode. We combined the two event analysers (EAs) of 2s readout time to reduce the Good Xenon data using the perl script MAKE_SE. Once the MAKE_SE script was run on the Good_Xenon_1 and Good_Xenon_2 pairs, the resulting file was reduced as an *Event* file using the SEEXTRCT script to extract light curves. Good time intervals were selected to exclude the occultations by the earth and South Atlantic Anomaly (SAA) passage and also to ensure the stable pointing. We also extracted energy spectra with an integration time of 16s from PCA Standard2 data in the energy range 3–30 keV (out of the five PCUs only data from No. 2 and No. 3 PCUs are added together). For each spectrum, we subtracted the background data that are generated using PCABACKEST v4.0. PCA detector response matrices are created using PCARSP v7.10. We performed fits to the energy spectra in the energy range 3–27 keV with the so-called 'traditional model' for SS 433, consisting of the super-position of thermal bremsstrahlung and Gaussian lines due to the emission from the iron atoms, modified by the interstellar absorption.

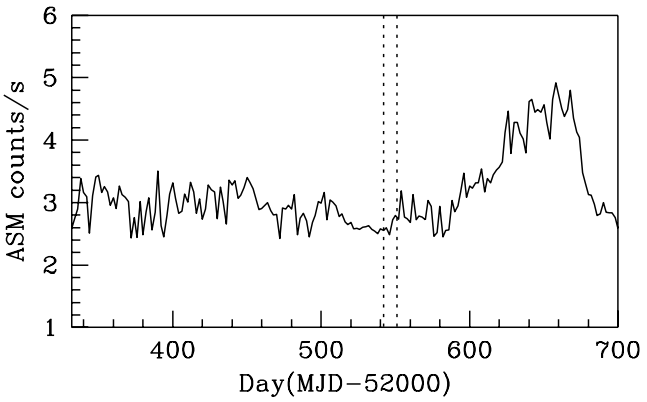

Figure 1. The average All Sky Monitor (ASM) light curve of SS 433 as taken by the *RXTE* satellite. The dotted vertical lines show the days of the present campaign, indicating that the object was expected to be X-ray quiet.

3 RESULTS AND DISCUSSIONS

Before we present the results of our campaign, we would like to give an overview of the long-term behaviour of SS 433 in X-rays (Nandi et al. 2005). Fig. 1 shows the average *RXTE* All Sky Monitor (ASM) data. The complete set of ASM data since 1996 till date has been averaged after folding it around 368 ± 3 d. This shows clear periodicity. This 'flaring' is the result of the special alignment of SS 433 with the sun as seen by the ASM every year. The vertical dashed lines represent the duration of our campaign, which took place during a time-frame in which the object was expected to be X-ray quiet. Because of this we expected that even small variations in intensities would be detectable.

In Fig. 2(a), we present the images of SS 433 obtained by our radio observation at 1.28 GHz on 2002 October 1. The contours are drawn at intervals of 0.055 Jy. The beam size is shown as a circle in the lower left. In Fig. 2(b) is shown the image of SS 433 on 2002 September 27, along with the those of the two standard stars in the J band. The magnitudes of the standard stars are also given.

Fig. 3 shows the results of our multi-wavelength observation of SS 433 at the 1.28-GHz band (triangles) and at 610 MHz (filled hexagons) in the radio, at J (crosses), H (filled boxes) and K' (filled pentagons) bands in the IR, B (filled circles) and V (open circle) bands in the optical, and 3–25 keV (open squares) in the X-ray during the campaign. There seems to be a minimum in the IR data on ∼MJD 52544.674 (see Fig. 5, and associated discussion, below) while the radio shows minimum at ∼MJD 52546.7, almost two days later. If the IR data could be taken as the pre-cursor of the radio data, one would infer that IR was also in a state of minimum intensity during the campaign. However, it is to be noted that this IR intensity could be the sum of the components coming from the companion and the jet. From the IR observation of Kodaira et al. (1985), one notices that at the precessional and orbital phases of SS 433 corresponding to our campaign, the relative K magnitude was expected to remain almost constant ($\sim 0 \pm 0.05$), while in our observation we find it to be highly variable (∼0.225) which suggests that there are

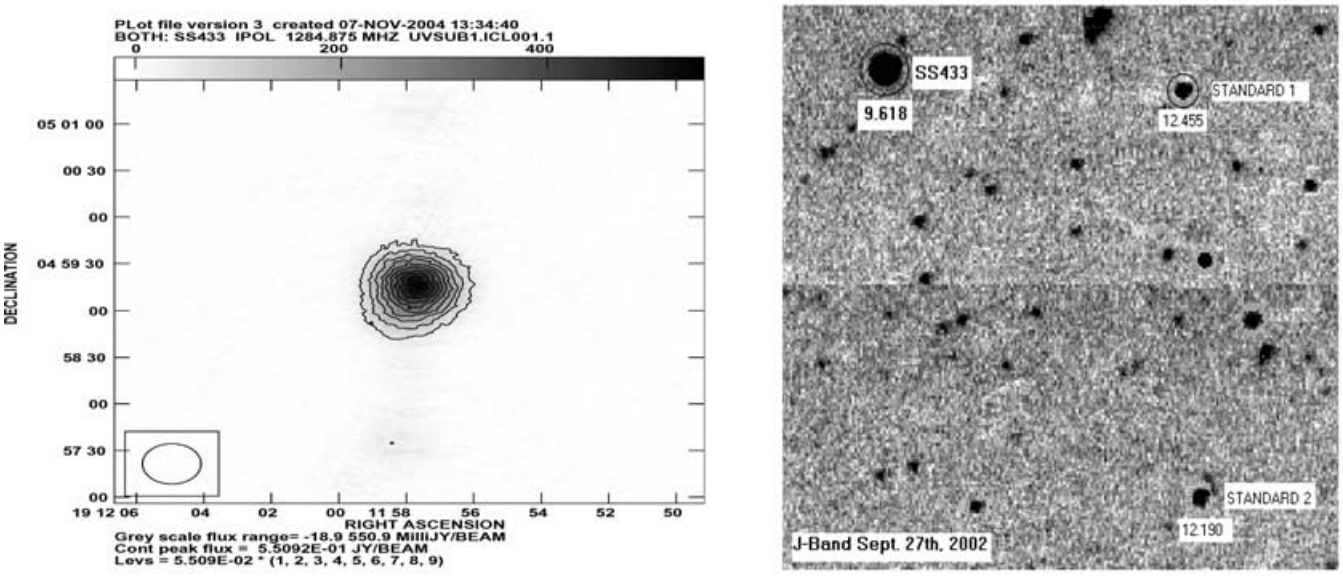

Figure 2. (a) Radio and (b) IR images of SS 433. This radio image taken on 2002 October 1 is at 1.28 GHz. The peak flux is $\sim$0.55 Jy beam^{-1}. The size of the beam is given in the lower left. The contours are at intervals of $\sim$0.055 Jy. The IR image taken on 2002 September 27 is in the *J* band. The standard stars (1 and 2) referred in the text are also shown. The magnitudes are given as well.

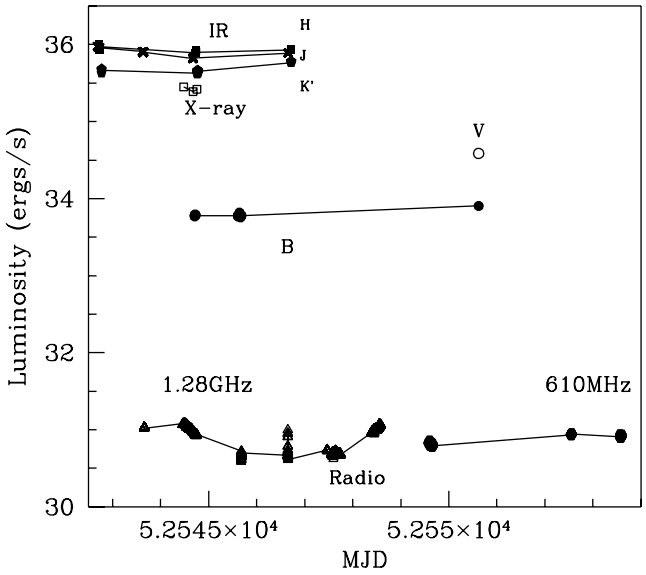

Figure 3. Multi-wavelength observation of SS 433 at 1.28 GHz (triangles) band and at 610 MHz (filled hexagons) in radio, at J (crosses), H (filled boxes), K' (filled pentagons) bands in IR, B (filled circles) and V (open circle) bands in optical, and 3–25 keV (open squares) in X-ray during the campaign. There seems to be a lag of minimum intensity region in the radio (MJD 52545.5 to MJD 52547.5) with respect to the infrared minimum region ($\sim$MJD 52544-52545) by about 2 d.

intrinsic variation in the IR band which may have been reflected in the radio band two days later. To obtain the precessional and orbital phases, we follow Gies et al. (2002) and Goranskii et al. (1998) respectively. The *H*-band result was found to be higher compared to the *J*- and K'-band results during the whole period. A similar result of turnaround at about 4 micron was reported earlier by Fuchs (2001 and citations therein). This turn over could be possibly due to the free–free emission in the optically thin limit. Absorption in the *J* band by the surrounding matter or the jets may also be a possibility. In Fig. 4 we present the multi-wavelength lightcurves in the radio (1.28 GHz), in the *J*-, *H*- and K'-bands, in the *B*-band and in X-rays (3–30 keV) obtained on 2002 September 27. The mean radio flux was seen to gradually go down while its behaviour in other wavebands was not so straightforward. The flux in *H* band is clearly seen to be higher compared to *J* or K' as discussed above.

In Fig. 5 we present the entire IR observations taken during the campaign. The flux is clearly diminishing during September 25–27, and has started rising again on September 29. The minimum is at around MJD 52544.674. Our high-frequency sampling (10 s) data is clearly variable on a time-scale of a few minutes (Chakrabarti et al. 2003). Such short time-scale variations, on the order of ten minutes, have also been reported earlier (Kodaira & Lenzen 1983). The IR variability could be better and more clearly represented by the differential photometry analysis of IR observations, and detailed procedures have been described in Section 2. In Fig. 6(a) (upper graph) the differential photometry in the *J*-band is presented while in Fig. 6(b) (lower graph) that in *H*-band is presented. In each graph, the upper panel shows a relative flux difference (Δ F) between SS 433 and one bright comparison star (std1) in the same frame while the lower panel represents the difference between two bright comparison stars (std1 and std2) in the same frame of the object. The typical 3σ errors in the *J* and *H* bands are shown for each day and the error-bar is computed considering the observation errors in two stars. The short-term variability is best seen in Fig. 6 on September 27 and 29 in the *J* band and September 27 in the *H* band, where we have monitored the source uninterruptedly over a period of about 20 min. To determine whether the target star SS 433 shows evidence for intrinsic variability, we define a robust estimation procedure. The root mean square (rms) differential flux variation in SS 433 light curves (upper panel) particularly on September 27 (in the *J* and *H* bands) and September 29 (in the *J*-band) was 2–3 times that of the comparison stars (lower panel). In Fig. 6, the *J*-band light curve on September 27 shows the rms scatter $\sigma_{\rm rms}$ (SS 433 - std1) $\approx$3.5 mJy while that for the comparison stars is $\sigma_{\rm rms}$ (std2-std1) $\approx$1.02 mJy; on September 29 $\sigma_{\rm rms}$ (SS 433 - std1) in the *J*-band $\approx$2.2 mJy while $\sigma_{\rm rms}$ (std2-std1)

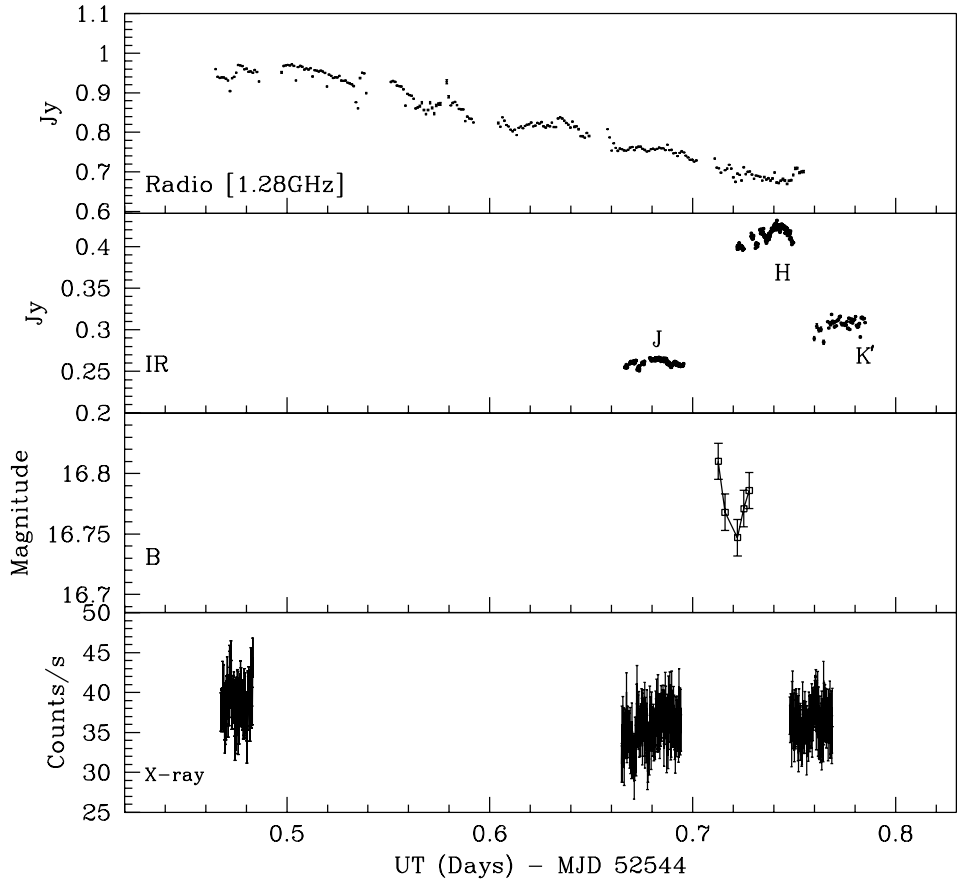

Figure 4. Light curves of SS 433 on the 2002 September 27, as obtained by our multi-wavelength campaign at different wavelengths. Upper panel: radio observation at 1.28 GHz at GMRT, Pune. Second panel: IR observation at J, H and K' bands at Mt. Abu. Third panel: B-band observation at the State Observatory, Nainital. Last panel: background subtracted X-ray count rates by the *RXTE* satellite.

$\approx$1.02 mJy; on September 27 $\sigma_{\rm rms}$ (SS 433 - std1) in the H-band $\approx$8.5 mJy while $\sigma_{\rm rms}$ (std2-std1) $\approx$3.5 mJy. Furthermore, we have also tested the intrinsic short-period variability in SS 433 following the statistical method of Howell et al. (1988) and find the significant variability in the source at a 95 per cent confidence level.

Since the optical results depended heavily on the local sky conditions, the data acquisition was not uninterrupted. Indeed, although two observatories, one in southern part of India (the VBT in Kavalur) and the other in the northern part of India (ARIES in Nainital) were chosen, both observations were affected by the late monsoon activities. Table 1 showed the duration of the data acquisition and the exposure time. In Fig. 7(a), the wavelength calibrated spectrum of 2002 September 27 is shown and major lines are identified. On this date, both the jets were showing redshifts. The shifted line wavelengths match with what is expected from the kinematic model of Abell & Margon (1979) within the instrument resolution of 5 Å. For example, at 13:49 UT, on 2002 September 27, the expected redshifts were 0.05901 and 0.01234 respectively and the $H_{\alpha-}$ and $H_{\alpha+}$ lines were expected at 6950 and 6644 Å respectively. Our observed lines were at 6961 $\pm$ 5 Å and 6642 $\pm$ 5 Å respectively. The red/blue shifted H_α lines had a very low intensity, indicating the decaying phase of the so-called optical bullets (Margon 1984; Vermeulen et al. 1993). The spectra on 2002 September 28, presented in Fig. 7(b), had two bright lines (marked by 'U' on the figure) at 7029 $\pm$ 5 Å and 6481 $\pm$ 5 Å respectively, apart from the usual lines. On this day, the spectrum was taken six times, and in all the spectra these two unidentified lines were seen with almost same location and line profiles. The origins of the bright 'U'-marked lines are not totally clear as they are not close to the $H_\alpha\pm$ lines expected on that day. These could arise out of the winds from the accretion disc. If this is correct, and these lines are identified as the blue and red-shifted H_α lines, then the projected velocity components along the line of sight required to produce these lines would be 21 300 $\pm$ 229 km s^{-1} (away from the observer) and 3748 $\pm$ 227 km s^{-1} (towards the observer) respectively. The ratios of the equivalent widths of these lines and that of the H_α line are 0.4 and 0.45 respectively. Thus, the emergence of these extra sources of winds are almost half as strong as the original source of H_α. On 2002 September 27, there was an unidentified line on the blue-ward side of the H_α line at 6503 $\pm$ 5 Å as well (corresponding to a velocity of 2742 $\pm$ 227 km s^{-1}). This is also marked as 'U' in Fig. 7(a). Abnormal activities in the jets may not be ruled out as explanations for these unidentified lines, in which case the asymmetry of the red and blue shifts would be the result of probable intrinsic redshifts of the relativistic system. Unfortunately, the spectrum on 2002 September 30 could not be used, as there was a focusing error in the telescope.

The three spells of X-ray data (see Fig. 4, bottom panel) were analysed separately. We found that, generally speaking, a two-line model with a thermal bremsstrahlung is necessary for a statistically and physically acceptable fit to the X-ray spectra. However, the significance depends on the duration of observation. In Fig. 8, we present the X-ray spectrum of the first spell of our *RXTE* observation. The single-line fit to the spectra yields $\chi^2/\nu = 44.94/45$ (ν is the total number of degrees of freedom) whereas the double-line fit

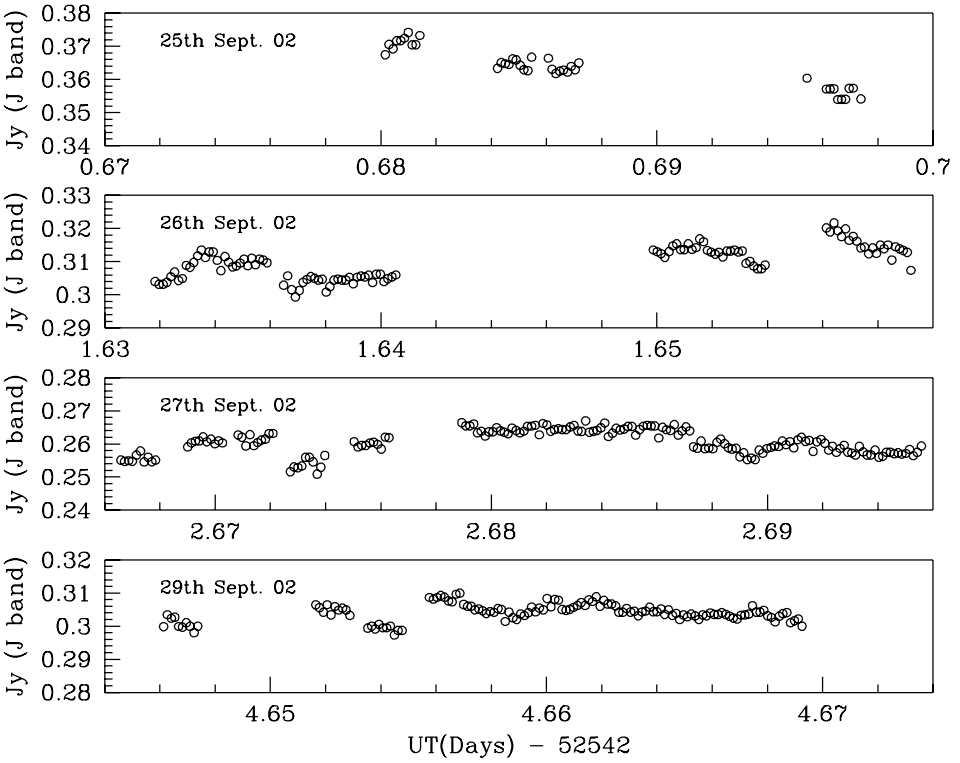

Figure 5. Light curves in the *J* band as a function of the UT (days). Considerable variations could be seen in all the days. The sizes of the error-bars are well below the sizes of the circles. The intensity seems to be minimum (around 0.25 Jy) on MJD 52544.674.

gives a more acceptable value with $\chi^2/\nu = 34.84/43$. The requirement of the second line in the spectrum is tested from the FTEST TASK within XSPEC, and it is found that the fit is significant at the 2.4σ level. The best-fitting two lines found at energies 6.966 ± 0.084 keV and 6.898 ± 0.084 keV correspond to the Doppler-shifted values of $z = -0.00014 \pm 0.012$ (Fe XXVI) and $z = -0.032 \pm 0.012$ (Fe XXV) or $+0.0096 \pm 0.0012$(Fe XXVI) respectively. The observed flux is 2.6524×10^{-10} erg cm^{-2} s^{-1} in the energy range $3 - 25$ keV with the bremsstrahlung temperature at 15.77 ± 0.53 keV. We failed to fit the spectrum with a model having a blackbody emission component. Thus, we did not find any evidence of a Keplerian disc. Similarly, the single-line fit to the spectra of the second spell of X-ray observation (Fig. 4) yields a $\chi^2/\nu = 54/45$ whereas a double-line fit gives more acceptable value with $\chi^2/\nu = 35.7/43$. The requirement of the second line in the spectrum is tested and it is discovered that the fit is significant at 3σ level. The best-fitting two lines are found at energies 7.012 ± 0.06 keV and 6.802 ± 0.072 keV, which correspond to the Doppler-shifted values of $z = -0.007 \pm 0.009$(Fe XXVI) and $z = -0.018 \pm 0.011$ (Fe XXV) respectively. Here too, both the lines are from the blue jet of SS 433. The observed flux is 2.375×10^{-10} ergs cm^{-2} s^{-1} in the energy range 3–25 keV with the bremsstrahlung temperature at 13.92 ± 0.34 keV.

Fig. 9 gives the broad-band spectrum of SS 433 that we obtained using our multi-wavelength campaign. Campaign average data has been used for simplicity. For the radio frequency, the 610 MHz and 1.28 GHz data have been used, while in the IR we used the results at the *I*, *J* and *K′* bands. We included *V*- and *B*-band observations which clearly show heavy extinction and in which the luminosity drops dramatically. The X-ray spectrum in $3 - 27$ keV is also shown. To compare with the results of others, we have included three observations at wavelengths which were not covered during our campaign (triangles). Thus, the 21.7-GHz observation of Trushkin et al. (2003), the ultra-violet observation of Dolan et al. (1997) and the gamma-ray observation of Cherepashchuk et al. (2003) have been included. These three points were not contemporaneous to our campaign, but they do generally fall at reasonable values in the overall spectrum.

Since we find no report of such a broad-band spectrum of SS 433 in the literature, it is difficult to know what to compare our results with. In the radio region we find that the slope is negative, i.e. the synchrotron radiation is in the optically thin regime and the self-absorption frequency is lower than 610 MHz. The data of Trushkin et al. (2003) also fall within our power-law radio spectrum. The IR emission in the western lobe of W50 was suggested to be due to synchrotron emission (Fuchs et al. 2001), although in the present case this identification could not be made, since (a) high-resolution imaging was not carried out to allow for visually suggesting a relation and (b) the spectral slope at IR is reversed and thus is not a natural extension of the radio spectra. From the variability in the time-scale of a few minutes, it seems that the IR emission is from a region far closer to the central object ($\sim 10^{12}$ cm) and the jet is emitted from a region farther out ($\sim 10^{15}$ cm). The optical data have not been corrected for extinction. If corrected, the emitted flux should be at par with the IR result or even higher. When compared with other microquasars, the X-ray flux is very low: indeed, the X-rays are known to be emitted mainly from the bases of the jets rather than from the accretion flows. The gamma-ray emission of Cherepashchuk et al. (2003) is in line with our X-ray observation.

If one looks at the prevalent models of a typical microquasar such as GRS 1915+105, one finds that SS 433 has very 'dull' X-ray features. No QPOs have been reported. Variabilities on time-scales of minutes or less indicate that the X-rays are emitted in regions

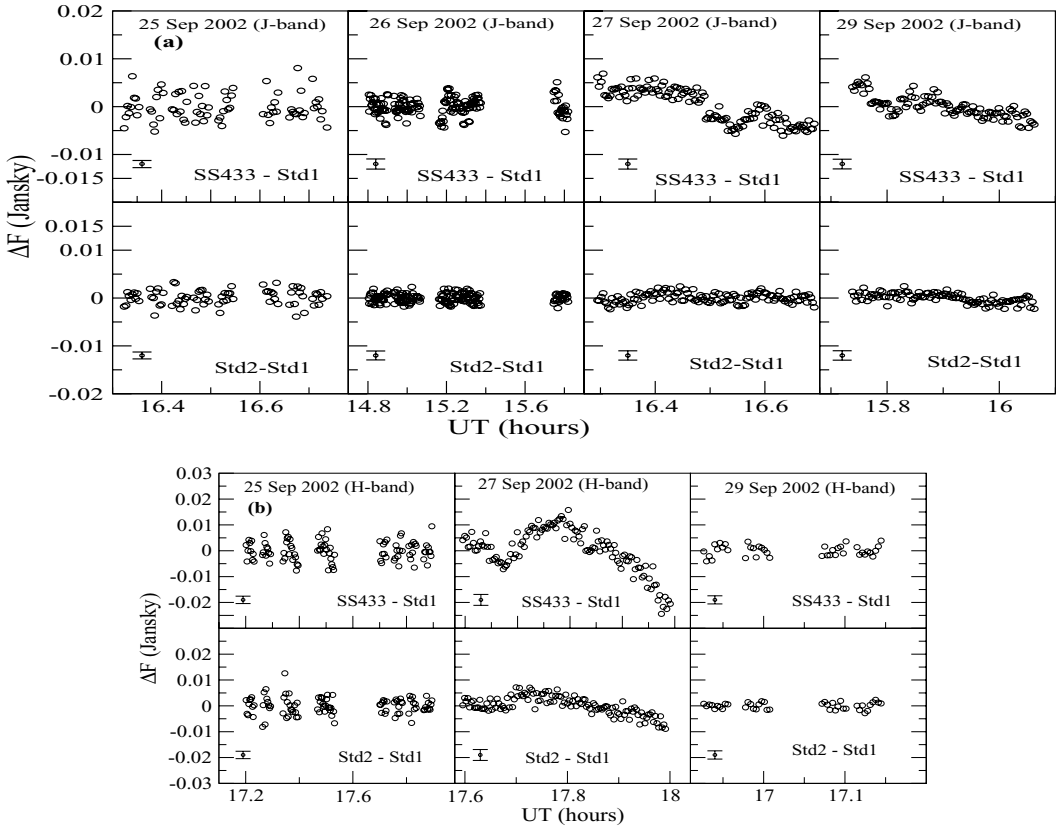

Figure 6. Differential photometry of SS 433 in IR J and H bands with respect to a comparison star (std1) in the same frame of the object are plotted against UT on various days of the campaign in the upper panel, while the photometry for the two comparison stars (std1 and std2) in the same frame of the object are plotted in the lower panel. The upper graphs are for J-band and lower graphs for H-band. The typical 3σ errors for differential measurements in both bands are plotted in each box. The rms differential flux variation in the SS 433 light curve is above the 2σ level of that in the comparison stars.

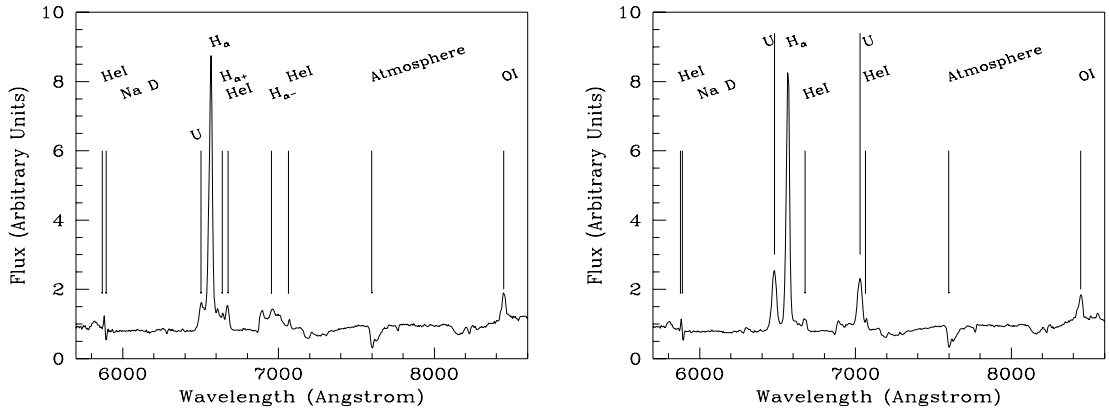

Figure 7. The calibrated, continuum-subtracted, optical spectrum of SS 433 on 2002 September (a) 27 and (b) 28. In (a) the H_α line, blue- and red-shifted H_α lines (denoted by $H_{\alpha+}$ and $H_{\alpha-}$ respectively), HeI lines, OI line, atmospheric and sodium absorption lines are identified. The Doppler-shifted H_α lines are exactly where there are expected from kinematic model of Abell & Margon (1979) within the instrumental resolution of 5 Å. In (b) we also see two bright lines, marked by 'U' at 7029.07 and 6481.09 Å respectively.

less than 10^{12} cm along the jets (see below). The presence of two iron lines whose Doppler shifts agree with that obtained from the kinematic model also confirm the jet-emission model.

4 CONCLUDING REMARKS

In this paper, we have presented results of a recent multi-wavelength campaign on SS 433 carried out during 2002 September 25 – October 6, using radio, IR, optical and X-ray instruments. The average ASM X-ray data indicated that the campaign was conducted when the X-ray intensity was low, which we also verify from our observations with PCA. We found that there is a tendency for the radio intensity variation to lag behind the IR variation by about two days. The broad-band spectrum clearly showed evidence of very high extinction in the optical region, possibly due to a large scale obscuration of the central object by matter coming from the companion wind (e.g. Paragi et al. 1999). The X-ray data could be fitted with two Fe lines, both of which appear to be coming from the blue-shifted jet,

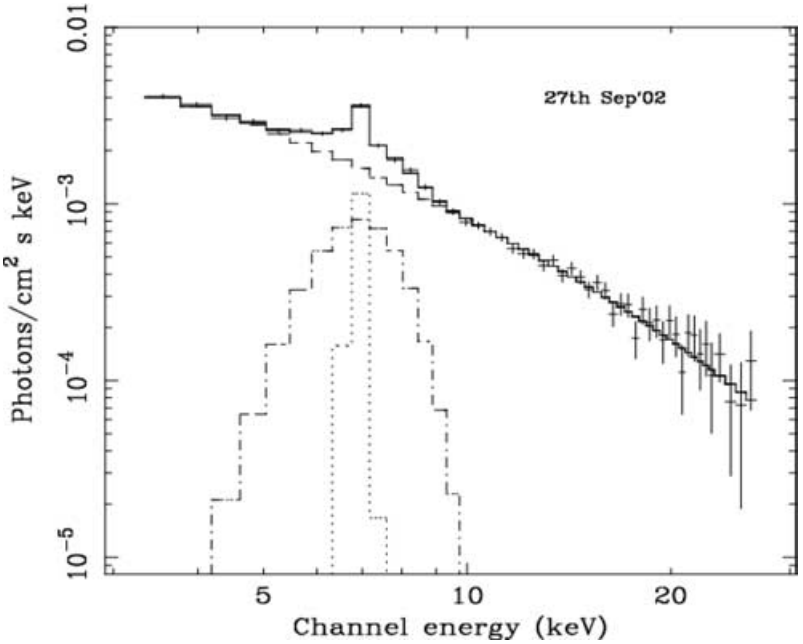

Figure 8. The X-ray spectrum of the first session of the *RXTE* observation of 2002 September 27. The spectrum was fitted with a bremsstrahlung and two iron lines (shown with dotted and dot dashed curves.)

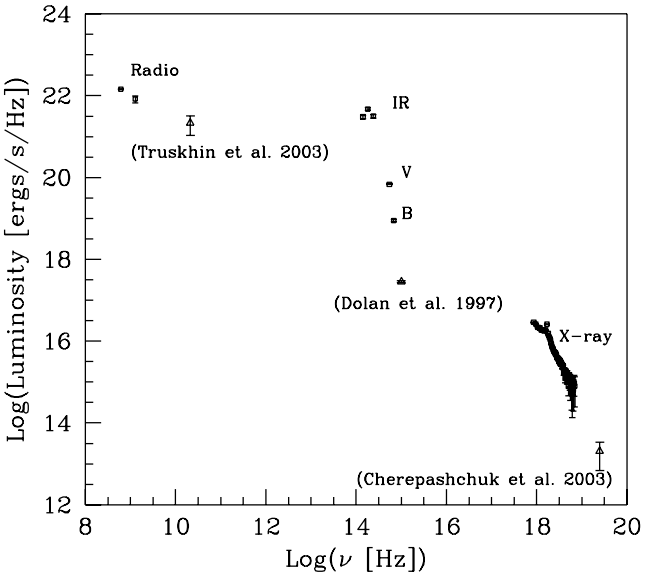

Figure 9. The multi-wavelength spectrum of SS 433 as obtained by our campaign. Here, average luminosity (open boxes) over our available data has been plotted and the wavebands are marked. For comparison, we include three points, marked by open triangles with error bars, from the literature (marked) which are not contemporaneous with our observation.

i.e. the jet pointing towards us. We also find very small time-scale (of the order of a few minutes) variations in all the wavelengths which could be suggestive of small bullets propagating from the base of the jet on the accretion disc to the radio regions, as originally suggested in our earlier communications (Chakrabarti et al. 2002, 2003). The differential photometry in the IR gives very clear indications that these short time-scale variations are intrinsic to the jet. In optical spectra we observed that the blue- and red-shifted H_α lines appeared almost at the predicted locations on 2002 September 27. On September 28, the intensities of these lines were very low, possibly because the so-called optical bullet emission was on the decaying phase. We also see two bright, unidentified lines in all the frames taken on September 28, which could be due to sudden winds in the companion. Our optical and X-ray spectra indicate that the kinematic model generally gives the correct description even today, more than 25 years after its discovery. To summarize our major results, we find that:

(a) the short time-scale variations are present (2–8 min) on all the days in all the wavelengths;

(b) the optical and X-ray spectra contain the displaced lines which are compatible with the kinematic model (Abell & Margon 1979);

(c) for the first time, we obtained the broad-band spectrum over ten decades of frequency range based on contemporaneous data and finally,

(d) the radio emission may be lagging behind the IR emission by as much as two days, i.e. the radio emission is at least $\sim 10^{15}$ cm away from the black hole.

SS 433 has always been a puzzle and it is still so even 25 years after its discovery. The mass estimate of the recent observation (Hillwig et al. 2004) is an indication that the central compact object could be a small-mass black hole. Given that in the last decade fresh understanding about the accretion processes onto black holes have emerged, it may be necessary to consider this system with a fresh approach. Our result gives some idea about the physical processes that are going on near the compact object.

(a) The X-ray spectrum does not show any indication of a Keplerian disc. Thus the flow may be totally sub-Keplerian or advective (Chakrabarti = 1990), as would be expected if the accretion is from winds.

(b) The broad-band spectrum indicated heavy extinction in the optical/UV region. This is to be expected from the matter that has accumulated around the system (Paragi et al. 1999).

(c) Short time-scale variations may indicate disc instabilities causing ejection of bullet-like entities, which could be formed due to

shock oscillations in the advective flows at the jet base (Chakrabarti et al. 2002).

(d) There is a general indication that the radio intensity follows the IR by about two days. This could not be rigorously confirmed as the coverages in the campaign were not very high. If correct, and if we assume that the same matter generally propagates from the IR jet to the radio jet, this would indicate that the radio emission takes place only about 1.3×10^{15} cm away from IR emitters. This seems to be quite reasonable. In fact, while comparing the results of Kodaira et al. (1985) with our observations, we conclude that there are intrinsic variations in the IR band which may have been reflected in the radio band two days later.

According to Brinkmann et al. (1991), the length of the X-ray jet is smaller than $\sim 10^{11}$ cm. In our analysis, we find the temperature of the X-ray emitting region to be $kT \sim 15$ keV which, using the model of Kotani et al. (1996), corresponds to an even smaller distance of $\sim 10^{10}$ cm. While analysing *RXTE* data from SS 433 for over two years, Nandi et al. (2005) found the temperature to be even higher. Therefore, the X-ray emission must be from a region much closer to the compact object. On the other hand, IR emission from the jet may be emitted somewhere around 10^{12-13} cm (Fuchs 2001), as is evident from our findings of the intrinsic variability also. Thus, the time lag between X-rays and IR should be at the most a few hundreds of seconds. Lack of continuous X-ray observation during our campaign does not allow us to make a definite comment on whether this lag was observed or not.

SS 433 is a treasure house of mystery. Even if one has to live with heavy extinction which blocks the disc features almost completely, one can assume the same solutions to be operating around similar compact objects, except that in the present case the sub-Keplerian accretion rate may be much higher than the Eddington rate because of its profuseness. However, in the last few years it has been established that the jets are produced from the innermost part of the sub-Keplerian disc where the matter is centrifugal-pressure dominated. Presence of a shock front, whether it is static, propagating or oscillating, will surely show its signature in the jets (Chakrabarti et al. 2002, 2003). We believe that bullets are signatures of such instabilities which must propagate along the jets. One exciting difference between GRS 1915+105 and SS 433 would be as follows: in GRS 1915+105 one would expect an anti-correlation between X-ray emission (a predominantly disc component) and radio emission when the innermost disc is evacuated (Nandi et al. 2001 and references therein) but in SS 433, where the jet itself is emitting X-rays, they should be correlated with a time lag. In future, we plan to carry out a larger multiwavelength campaign on SS433 which will show correlations with time lags depending on the emission frequencies.

ACKNOWLEDGMENTS

SKC thanks Dr J. Swank of NASA/GSFC for arranging TOO time of *RXTE*. We thank the staff of the GMRT who have made these observations possible. GMRT is run by the National Centre for Radio Astrophysics of the Tata Institute of Fundamental Research. This work is supported in part by CSIR fellowship (SP), a DST project (AN) and an ISRO project (S. Mandal).

REFERENCES

Abell G. O., Margon B., 1979, Nat, 279, 701
Band D. L., Gordon M. A., 1989, ApJ, 338, 945
Bessell M. S., Castelli F., Plez B., 1998, A&A, 333, 231
Brinkmann W., Kawai N., Matsuoka M., Fink H. H., 1991, A&A, 241, 112
Chakrabarti S. K., 1990, Theory of Transonic Astrophysical Flows. World Scientific, Singapore
Chakrabarti S. K., Goldoni P., Wiita P. J., Nandi A., Das S., 2002, ApJ, 576, L45
Chakrabarti S. K., Pal S., Nandi A., Anandarao B. G., Mondal S., 2003, ApJ, 595, L45
Cherepashchuk A. M., Sunyaev R. A., Seifina E. V., Panchenko I. E., Molkov S. V., Postnov K. A., 2003, A&A, 411, 441
Ciatti F., Mammano A., Bartolini C., Guarnieri A., Piccioni A., Downes A. J. B., Emerson D. T., Salter C. J., 1981, A&A, 95, 177
Corbel S., Nowak M. A., Fender R. P., Tzioumis A. K., Markoff S., 2003, A&A, 400, 1007
Dolan J. F. et al., 1997, A&A, 327, 648
Eikenberry S. S., Matthews K., Morgan E. H., Remillard R. A., Nelson R. W., 1998, ApJ, 494, L61
Elias J. H., Frogel J. A., Matthews K., Neugebauer G., 1982, AJ, 87, 1029
Fuchs Y., 2001, PhD thesis, Service d'Astrophysique, CEA/SACLAY, Gif-sur-Yvette
Fuchs Y., Mirabel I. F., Ogley R. N., 2001, Ap&SS, 276, 99
Fuchs et al., 2003, A&A, 409, 35
Gies D. R., McSwain M. V., Riddle R. L., Wang Z., Wiita P. J., Wingert D. W., 2002, ApJ, 566, 1069
Glass I. S., 1979, in Marsden B. G., ed., IAU Circ. 3363.
Goranskii V. P., Esipov V. F., Cherepaschuk A. M., 1998, Astron. Rep., 42, 209
Hillwig T. C., Gies D. R., Huang W., McSwain M. V., Stark M. A., van der Meer A., Kaper L., 2004, ApJ, 615, 422
Homan J., Buxton M., Merkoff S., Bailyn C. D., Nespoli E., Belloni T., 2005, ApJ, 624, 295
Howell S. B., Mitchell K. J., Warnock A., III, 1988, AJ, 95, 247
Kodaira K., Lenzen R., 1983, A&A, 126, 440
Kodaira K., Nakada Y., Backman D. E., 1985, ApJ, 296, 232
Kotani T. et al., 1999, Astron. Nachr., 320, 335
Kotani T., Kawai N., Matsuoka M., Brinkmann W., 1996, PASJ, 48, 619
Margon B., 1984, ARA&A, 22, 507
Milone E. F., Clark T. A., 1979, in Marsden B. G., ed., IAU Circ. No. 3354
Nandi A., Chakrabarti S. K., Belloni T., Goldoni P., 2005, MNRAS, 359, 629
Nandi A., Chakrabarti S. K., Vadawale S., Rao A. R., 2001, A&A, 380, 245
Neizvestnyj S. I., Pustilnik S. A., Efremov V. G., 1980, Sov. Astron. Lett., 6, 368
Paragi Z., Vermeulen R. C., Fejes I., Schilizzi R. T., Spencer R. E., Stirling A. M., 1999, A&A, 348, 910
Prabhu T. et al., 1995, A&A, 295, 403
Revnivtsev M. et al., 2004, A&A, 424, L5
Seaquist E. R., Gilmore W. S., Johnston K. J., Grindlay J. E., 1982, ApJ, 260, 220
Swarup G., Ananthakrishnan S., Kapahi V. K., Rao A. P., Subrahmanya C. R., Kulkarni V. K., 1991, Current Science, 60, 95
Trushkin S. A., Bursov N. N., Smirnova J. V., 2003, in Durouchaux P., Fuchs Y., Rodriguez J., eds, New Views of Microquasars. Centre for Space Physics, Kolkata, p. 283
Ueda Y. et al., 2002, ApJ, 571, 918
Vermeulen R. C., 1989, Multi-wavelength studies of SS 433, PhD thesis, Rijksuniversiteit, Leiden
Vermeulen R. C., McAdam W. B., Trushkin S. A., Facondi S. R., Fiedler R. L., Hjellming R. M., Johnston K. J., Corbin J., 1993, A&A, 270, 189

This paper has been typeset from a TEX/LATEX file prepared by the author.